

$$c_n = \frac{1}{2 \cdot 2^{n-1}} c \quad (1)$$

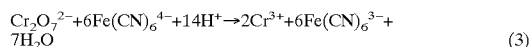
[0151] Channel n=1 corresponds to the channel that contains the solution injected into inlet 344 (0% dilution). Channel n=11 corresponds to the channel that contains 100% of the solution injected into inlet 346, i.e., this solution flows to the end of the device without being mixed with any solution from inlet 344.

[0152] In the case of potentiometric measurements, if a redox-active species (a reductant R, for example) is injected into inlet 344, the potentials measured in each channel follow the Nernst equation and are therefore proportional to the logarithm of the concentration in each channel, i.e.,  $E \propto \ln(c)$ , if the concentration of the oxidant is kept constant. The relationship between E and n is thus linear for the case of these channels for a constant concentration of oxidant (eq. 2).

$$E_n = E^\circ + \frac{RT}{\alpha F} \ln(c_{O_x}) - \frac{RT}{\alpha F} \ln(c) + \frac{RT}{\alpha F} \ln(2.2)^{(n-1)} \quad (2)$$

[0153]  $C_{O_x}$  is the constant concentration of the oxidant,  $\alpha$  the number of electrons exchanged between the reductant and the oxidant,  $E^\circ$  the formal redox potential of the oxidoreductant couple, R the gas constant, T the temperature, and F the Faraday constant. Thus, an exponential concentration gradient of a redox species results in a linear gradient of the electrochemical potential.

[0154] The redox systems Fe(II)/Fe(III) and Cr(III)/Cr(VI) was investigated in the microfluidic device shown in FIG. 27. The redox reaction between Cr(VI) ( $Cr_2O_7^{2-}$ , considered here as the titrant) and Fe(II) ( $Fe(CN)_6^{4-}$ , considered as the sample) is summarized by eq. 3:



[0155] The network offered two injection schemes: i) the case where the sample was injected into inlet 344 and the titrant into inlet 346, and ii) the reverse case, where the titrant was injected into inlet 344 and the sample into inlet 346. Results indicate that the choice of the injection scheme has an influence on the detection limit of the device.

[0156] First, a solution of Fe(II) (100 mM) was injected into inlet 344 and a titrant solution of Cr(VI) was injected into inlet 346. In order to have an optimal determination of the sample concentration, the dilution ratio exhibiting a titration end-point (i.e., the point in the titration where 99% of the sample has reacted with the titrant) may be located in one of the middle channels (i.e.,  $3 < n < 8$ ). The location of the titration end-point depends on the relative concentrations of the sample and the titrant.

[0157] Three different concentrations of Cr(VI)—0.05, 0.5 and 50 mM—were tested in order to demonstrate the influence of this parameter on the location of the titration end-point in the channel. FIG. 31A shows the potentials measured in each channel relative to a common Ag/AgCl reference electrode; the data are plotted against the channel number, n.

[0158] Since the representation E vs. n (FIG. 31A) may not allow a straightforward recognition of the titration end-point, and because a sigmoidal shape is more convenient for determining this point, a function defined by eq. 4 was applied to the experimentally measured potentials. Here,  $E_{\min(Fe)}$  is the potential measured when the solution of the sample contains only Fe and no Cr (that is, in channel 1),  $E_{\max(Cr)}$  is the potential measured when the solution of the titrant contains only Cr and no Fe (that is, in channel 11) and n ranges from values of 2 to 10.

$$\phi_n = \ln \left[ \left( \frac{E_{\min(Fe)} - E_{\max(Cr)}}{E_n - E_{\max(Cr)}} \right) - 1 \right] = \ln \left[ \left( \frac{E_1 - E_{11}}{E_n - E_{11}} \right) - 1 \right] \quad (4)$$

[0159] This mathematical expression is derived from the sigmoid function, eq. 5, which gives a sigmoidal relationship between any parameters y and x;  $A_1$  and  $A_2$  are two constants defining the minimum and the maximum values that can be reached by y,  $x_o$  is the abscissa corresponding to the mid-point between  $A_1$  and  $A_2$ , and dx is a normalizing factor.

$$y = \frac{A_1 - A_2}{1 + e^{\frac{(x-x_o)}{dx}}} + A_2 \quad (5)$$

[0160] Eq. 5 can be rewritten as eq. 6 when applied to this data set, where n ranges from values of 2 to 10:

$$E_n = \frac{E_{\min} - E_{\max}}{1 + e^\phi} + E_{\max} = \frac{E_1 - E_{11}}{1 + e^{\phi_n}} + E_{11} \quad (6)$$

[0161] Eq. 4 allows the redistribution of the experimental points between a maximum and a minimum value. In eq. 4, when the function  $\phi$  equals 0, the potential corresponds to the inflexion point of the sigmoid, i.e., the end-point of the titration.

[0162] FIG. 31B shows the sigmoidal representations of the experimental points presented in FIG. 31A that were obtained using this transformation. For the case of a 0.5 mM solution of Cr(VI) and a 100 mM solution of Fe(II), the titration end-point (which we call the “experimental end-point”) corresponded to channel 7, in good agreement with the titration end-point determined by calculations (the “theoretical end-point”). Table 1A summarizes the influence of the relative concentrations between the titrant and the sample on the titration end-point. Table 1A also shows comparisons between experimental and theoretical end-points for three different Cr(VI) concentration values. These results illustrate that the channel number where the titration end-point was determined experimentally shifted in agreement with the calculations.

[0163] The injection scheme described above could only detect a high concentration of sample (Fe(II), ~100 mM) and would require titrating against a very low concentration of Cr(VI) (<0.05 mM) to reach a lower detection limit of Fe(II). In order to decrease this detection limit, a second injection scheme was evaluated by injecting the sample Fe(II) into